

Original Article

Asian Pacific Journal of Tropical Biomedicine

apjtb.org

doi: 10.4103/apjtb.apjtb_395_24

Phytochemical profiling and anticancer potential of *Cymbopogon citratus* extract

Bader O. Almutairi✉, Mikhlid H. Almutairi, Badr A. Al-Dahmash, Saad Alkahtani, Saud Alarifi, Ahmed Rady✉

Department of Zoology, College of Science, King Saud University, P.O. Box 2455, Riyadh 11451, Saudi Arabia

ABSTRACT

Objective: To evaluate the anticancer potential of *Cymbopogon citratus* extract.

Methods: GC-MS analysis was used to identify phytocomponents in the methanolic extract of *Cymbopogon citratus*. A fractionation method was employed to isolate and assess the bioactivity of different fractions and their cytotoxic activities against cancer cell lines HCT116, LoVo, Caco-2, and HT-29 were investigated. A dual staining method with acridine orange and ethidium bromide was used to assess the effect of the extract on cell apoptosis. Additionally, the expression levels of *Bax* and *TP53* were quantified using real-time PCR in Caco-2 cells treated with the ethyl acetate fraction of *Cymbopogon citratus* extract. A protein array was employed to profile key pro- and anti-apoptotic proteins in Caco-2 cells. Moreover, molecular docking studies were conducted to investigate the interactions between key compounds of *Cymbopogon citratus* extract and specific apoptosis-related protein domains (PDB IDs: 7wql and 4bkx).

Results: A significant growth inhibition was observed in Caco-2 cells treated with *Cymbopogon citratus* extract. Among the seven fractions of the plant extract, the ethyl acetate fraction showed the highest cytotoxicity against Caco-2 cells with an IC_{50} value of (6.16 ± 0.01) μg/mL. The immunofluorescence assay showed that the ethyl acetate fraction could induce apoptosis of Caco-2 cells. Moreover, the fraction upregulated the gene expressions of *Bax* and *TP53* in a dose-dependent manner. The docking analysis demonstrated the interaction of five compounds isolated from the ethyl acetate fraction with key proteins in Caco-2 cells, indicating their anticancer properties.

Conclusions: *Cymbopogon citratus* extract shows anticancer activity against Caco-2 cells by inducing apoptosis. It may be a promising candidate for the treatment of colon cancer, which needs further investigation.

KEYWORDS: *Cymbopogon citratus*; Anticancer; Caco-2 cell; Apoptosis; Colon cancer

1. Introduction

Cancer stands as a prominent contributor to untimely fatalities on a worldwide scale, and its impact is projected to increase twofold by 2070 compared to 2020 statistics. This surge is expected to result in approximately 34 million new cases in 2070, marking a substantial rise from the numbers reported in 2018. These shifts may be ascribed to multiple elements, including population senescence, overall population growth, and evolving regional patterns[1]. In 2015, colorectal cancer was the third most frequent cancer in men and the second most prevalent cancer in women; approximately 1.9 million new cases were reported globally[2]. Colorectal cancer is the second leading cause of cancer-related deaths worldwide. It is responsible for approximately 935 000 deaths and constitutes 11% of all cancer diagnoses[3]. Variations in both the frequency and lethality rate of colorectal cancer are evident among countries, as per

Significance

Colorectal cancer remains a major global health issue, with limited natural treatment options available. Previous research has explored various plant extracts for anticancer properties, but few have demonstrated comprehensive activity against multiple cancer cell lines. This study shows that *Cymbopogon citratus* extract can inhibit Caco-2 cell viability and induce cell apoptosis by upregulating apoptosis-related proteins, highlighting *Cymbopogon citratus* extract as a promising source for natural cancer therapies.

✉To whom correspondence may be addressed. E-mail: bomotairi@ksu.edu.sa (BO. Almutairi); ahabdo@ksu.edu.sa (A. Rady)

This is an open access journal, and articles are distributed under the terms of the Creative Commons Attribution-Non Commercial-ShareAlike 4.0 License, which allows others to remix, tweak, and build upon the work non-commercially, as long as appropriate credit is given and the new creations are licensed under the identical terms.

For reprints contact: reprints@medknow.com

©2024 *Asian Pacific Journal of Tropical Biomedicine* Produced by Wolters Kluwer-Medknow.

How to cite this article: Almutairi BO, Almutairi MH, Al-Dahmash BA, Alkahtani S, Alarifi S, Rady A. Phytochemical profiling and anticancer potential of *Cymbopogon citratus* extract. Asian Pac J Trop Biomed 2024; 14(10): 448-460.

Article history: Received 9 July 2024; Revision 14 August 2024; Accepted 5 October 2024; Available online 28 October 2024

the GLOBOCAN 2020 data. Projections suggest that by 2035, the combined mortality rates for rectal and colon cancer will increase by approximately 60% and 71.5%, respectively[4]. The need for innovative therapies to combat this deadly disease continues. The scientific and research communities are increasingly focusing on naturally derived compounds due to their potential for fewer toxic side effects when compared to conventional treatments, such as chemotherapy[5].

Within the plant kingdom, naturally occurring secondary metabolites have garnered attention for their potential anti-cancer properties, paving the way for the creation of new pharmaceuticals. As these compounds find success and become established in cancer treatment, there is a growing emergence of new technologies to further advance this field[6]. Various types of cancer in humans exhibit common characteristics or genetic traits, including resistance to growth-inhibiting signals, enabling unrestricted replication. Cancer cells evade apoptosis and sustain angiogenesis within tumor tissues, facilitating their survival. Compounds derived from plants have shown promise in inhibiting cancer cell functions, such as impeding cell proliferation and triggering apoptotic cell death[7]. Phytochemical compounds from *Erythrina suberosa*, a decorative tree found in several Asian countries, have been studied[8]. 4′-Methoxy licoflavanone and alpinumisoflavone isolated from this plant exhibited potent cytotoxicity against human leukemia HL-60 cells. These flavonoids induced apoptosis through both extrinsic and intrinsic pathways, involving multiple molecular mechanisms, while also inhibiting key signaling pathways like NF-κB and STAT.

Plant-based compounds exhibit promising anticancer potential through various mechanisms such as counteracting free radicals[9], inhibiting cell proliferation, inducing apoptosis, and targeting key molecular pathways[10,11]. For example, compounds like allicin has shown efficacy in suppressing tumor growth, enhancing radiosensitivity, and modulating pathways crucial for cancer cell survival and metastasis[12–15]. Also, bromelain exhibited significant anticancer potential by modulating key genes related to programmed cell death[16,17], inhibiting cancer cell proliferation and metastasis through various pathways, and interfering with cell cycle regulatory proteins[18,19]. Additionally, bromelain's effects on critical signaling pathways like MAPK and NF-κB contribute to its anticancer properties, along with its antiangiogenic effects on VEGF[20,21].

Cymbopogon citratus (*C. citratus*), commonly known as lemongrass, is an aromatic plant belonging to the Gramineae family. The delightful scent of this herb is due to citral, a cyclic monoterpene that imparts a lemony aroma[15]. Originating in Asia, Africa, and the Americas, this perennial grass is widely dispersed. It is renowned for its abundance of essential oils, flavonoids, phenolic compounds, and other chemical compounds, which confer a broad spectrum of pharmacological benefits, including anti-obesity, antibacterial, antifungal, antinociceptive, antioxidant, antidiarrheal, and anti-inflammatory effects. *C. citratus* has a well-established history of use in folk and Ayurvedic medicine[12]. Scientific research has documented numerous beneficial properties of *C. citratus*, including its anti-inflammatory, cardioprotective, antibacterial, antioxidant, and antifungal properties[13,22]. Additionally, it has been recognized for its potential to mitigate conditions such as platelet disorders[16].

This research aimed to identify and profile the chemical constituents of *C. citratus* through GC-MS analysis and fractionation methods, to evaluate the cytotoxic effects of the plant extract on various cancer cell lines and confirm the molecular mechanisms underlying its anticancer properties using *in silico* studies.

2. Materials and methods

2.1. Collection of plant materials

C. citratus (KSU No:10242) a member of the Poaceae family, is a perennial herb characterized by tiny, long, needle-like leaves. Indigenous to regions such as Alexandria in Egypt, this plant underwent a thorough cleansing process with distilled water prior to being freeze-dried for extraction. The drying procedure was conducted in a controlled environment featuring dry conditions and minimal exposure to light. Subsequently, the dried *C. citratus* plant material was finely ground into a powder using a mixer mill (Retsch MM400, Germany), to ensure sample integrity. To maintain the long-term viability and integrity of the collected *C. citratus* specimens for future research and analysis, they were stored at an ultra-low temperature of −20 ℃.

2.2. Extract preparation

A 20 g portion of ground *C. citratus* extract (CCE) sample was subjected to maceration in 200 mL of 95% (*v/v*) methanol 70% (Fisher Scientific, Ltd.) at 30 ℃, with continuous agitation at 150 rpm for 24 h. Following maceration, the suspensions were filtered through Whatman filter paper, and any remaining residue underwent a second extraction and filtration using the same process. The resultant filtrates from both extractions were combined and concentrated using a rotary evaporator (Rotavac Heidolph), maintaining a temperature of 40 ℃. The concentrated filtrate, referred to as the methanol crude extract for CCE, was weighed and dissolved in methanol to achieve a final concentration of 10 mg/mL. These extracts were stored at −20 ℃ for future use. The bioactivity of the crude extracts was then assessed by exploring their potential bioactive properties.

2.3. Chemical component separation techniques

Several chromatographic techniques were used to separate and identify the bioactive compounds responsible for the observed

bioactivity. These methods encompassed the use of silica gel column chromatography and gas chromatography, enabling a comprehensive exploration of the chemical components to unravel their specific roles in observed bioactivity.

2.3.1. Column chromatography fractionation of CCE

This process aimed to fractionate the crude methanol extract of CCE, facilitating a detailed analysis of its constituents. Silica gel column chromatography was used to obtain semi-pure fractions from the most active crude extract. A slurry of silica gel, which served as the stationary phase for adsorbing the compounds to be separated, was meticulously packed into a 20 mm diameter column. Various eluents were utilized as the mobile phase, including hexane, a hexane-dichloromethane mixture (50:50), dichloromethane, a dichloromethane-ethyl acetate mixture (50:50), ethyl acetate, an ethyl acetate-methanol mixture (50:50), methanol, and acetic acid. Fractions were collected, concentrated with a rotary evaporator, re-dissolved in methanol to a concentration of 10 mg/mL, and stored at −20 ℃ for future use.

2.3.2. CCE phytochemical profiling

CCE phytochemical profiling was conducted using Gas Chromatography-Mass Spectrometry (GC-MS) with the Shimadzu GCMS-QP2020 system from Tokyo, Japan. An Rtx-1MS fused bonded column (dimensions: 30 m length, 0.25 mm inner diameter, and a film thickness of 0.25 μm) manufactured by Restek, USA, was utilized for the chromatographic separation. Helium served as the carrier gas, flowing at a rate of 1.41 mL per minute. The liquid sample was introduced into the heated injection chamber at 250 ℃ with a split ratio of 1:15. The column temperature was set to 45 ℃ for 2 min and then increased to 300 ℃ at a rate of 5 ℃ per minute. The mass spectrometer was set to an ion source temperature of 200 ℃, an ionization voltage of 70 eV, and a filament emission current of 60 mA. The ionization spectra were compared with the library and reference data from the National Institute of Standards and Technology to identify the individual compounds separated during the analysis[17].

2.4. Biological analysis

2.4.1. Cell culture

HCT116, LoVo, Caco-2, and HT-29 cell lines were obtained from Vacsera, cultured, and maintained until reaching 80%-90% confluence. The subcultivation process involved washing the cells with a 1× PBS solution and trypsinization. These cells were subcultured in 25 cm^3 cultivation flasks, utilizing 10% FBS Dulbecco's Modified Eagle Medium (DMEM). Following subcultivation, the flasks were then incubated in a 5% CO_2 environment at 37 ℃ until they reached the desired confluence.

2.4.2. Determination of cytotoxicity by MTT assay

The principal objective was to evaluate the bioactivity of the raw botanical extract using a growth inhibition assay on HCT116, LoVo, Caco-2, and HT-29 cell lines. Subsequently, additional experiments were carried out on the most potent crude sample and its corresponding fractions including hexane, a hexane-dichloromethane mixture (50:50), dichloromethane, a dichloromethane-ethyl acetate mixture (50:50), ethyl acetate, an ethyl acetate-methanol mixture (50:50), methanol, and acetic acid. Moreover, the study determined IC_{50} values and specifically evaluated the cytotoxicity of these fractions against Caco-2 cell lines using MTT assays at 595 nm with a microplate reader (SunRise, TECAN, Inc., USA). The growth inhibition assay was conducted in 96-well plates, following the method described by Mosmann[9]. Two separate plates were used for the MTT assay. In the dilution plate, each plant crude extract (50 μL) was diluted in 100 μL of DMEM and serially diluted across rows. The concentrations ranged from 6.3 ng/mL to 1.111 mg/mL. Methanol served as the vehicular control, and all treatments were replicated and appropriately labeled. In the cultivation plate, 5×10^4 cells/mL of the cell lines were seeded (120 μL) in 96-well plates and treated with 60 μL from the diluted treatments prepared in the dilution plates. After 4 days of incubation in a CO_2 incubator, 20 μL of MTT salt was added. Following a 2-hour incubation, the MTT salt produced formazan crystals. The solution was gently aspirated with a vacuum aspirator to preserve the formazan crystals. Formazan was then dissolved in isopropanol and incubated for an additional 10 min. Following placement on a shaker for 10 min, the optical densities were assessed at 595 nm using a plate reader. The outcomes are expressed as a relative percentage compared to the control value and were determined by identifying the concentration at which cell proliferation was reduced by 50%, denoted as IC_{50}, using Origin 8 software. Each compound was subjected to triplicate testing.

2.4.3. Determination of apoptosis by immunofluorescence staining

The dual staining method employing acridine orange (AO) and ethidium bromide (EB), as outlined by Liu *et al.*[19], was conducted as follows: cells were seeded in a 96-well plate at a density of approximately 10^4 cells per well. After 48 hours of incubation with the ethyl acetate fraction, the cells were subjected to trypsinization and the subsequent transfer of cell suspensions ranging from 10 to 25 μL onto glass slides. One microliter of AO/EB staining solution, which is a mixture of dyes containing 100 μg/mL AO and 100 μg/mL EB, was added to the cell suspensions, and the samples were covered with a coverslip. Cell morphology was observed using a fluorescent microscope (Carl-Zeiss/Axio observer 3, Zen 2.3 Blue Edition software) within 20 min after the addition of the AO/EB stain. For statistical analysis, a minimum of 200 cells were counted and photographed, and the results represent the mean values obtained from at least three independent experiments. In this assay,

both live and dead cells were stained with AO, and EB exclusively stained dead cells that had lost membrane integrity. Viable cells display consistent green fluorescence, whereas apoptotic cells exhibit an orange staining pattern and condensed or fragmented nuclei.

2.4.4. Isolation of RNA

The objective of this investigation was to extract RNA from Caco-2 cells treated with the ethyl acetate fraction, followed by purification and quantification of the RNA for the analysis of gene expression. Caco-2 cells were exposed to the ethyl acetate fraction at 1, 2.5, and 5 times the IC_{50} value (6.16 µg/mL) and methanol as a control, for 24 h in duplicate samples. Treated and untreated cells were harvested as pellets through trypsinization and centrifugation (5 min at 300 ×*g*). RNA was isolated following the RNeasy Mini Kit protocol. In brief, the cellular suspension was mixed with 350 µL of lysis buffer and then agitated vigorously for 1 min using a vortex mixer. An equal volume of 70% ethanol was added, and the solution was thoroughly mixed by pipetting. Subsequently, 700 µL of the lysates were loaded onto RNeasy spin columns with collection tubes. After centrifugation, the spin columns were washed twice before the RNA was eluted with nuclease-free water. The isolated RNA was then checked for purity, quantified using a NanoDrop 8000 spectrophotometer (Thermo Fisher Scientific, USA), and stored at −80℃ until further use.

2.4.5. Gene expression assay

The expression levels of crucial apoptosis-related genes including *Bax* and *TP53*, were determined in Caco-2 cells. This assessment was conducted after subjecting the cells to a 2-day treatment with CCE ethyl acetate fraction at 37℃. Real-time PCR analyses were carried out using the Thermo Fisher Quantstudio 5 0.1 ML system to determine the gene expressions, comparing control samples without treatment to both untreated and treated cells exposed to varying doses of CCE ethyl acetate fraction. Total RNA extraction was carried out using the RNeasy Mini Kit from Qiagen (Hilden, Germany), and cDNA was synthesized from 1 µg of RNA using the Sigma-Aldrich cDNA synthesis kit (product no. 11117831001, Germany). In the qRT-PCR procedure, 10 ng of cDNA was used, with an initial heating phase of 5 min at 95℃. Subsequently, 45 cycles were conducted, involving denaturation at 95℃ for 10 s, annealing at 60℃ for 30 s, and extension at 72℃ for 1 min each, employing the iScript™ One-Step RT-PCR Kit with SYBR® Green (Bio-Rad, Hercules, California, United States). Subsequently, we determined relative gene expression using the $2^{-\Delta\Delta CT}$ equation and normalized the data to the reference gene *GAPDH* (Table 1)[23].

2.5. Protein array

A potential pathway of apoptosis triggered by the extract of *C. citratus* in Caco-2 cells was examined using a protein profiler array (RayBio, Human Apoptosis Antibody Array C1 Kit) to detect the expression of apoptosis-related proteins. The cells were exposed to 5 times the IC_{50} value (6.16 µg/mL) of the CCE ethyl acetate fraction for 24 h. Bradford's reagent was used to determine the concentration of protein in the samples. Proteins (240 µg) were extracted from the three exposed and control cells and then incubated overnight with the human apoptosis antibody array[24].

Image Lab (6.0) software was used to quantify the apoptosis array data of the membranes using Bio-Rad ChemiDoc XRS+ equipment. After examining the membrane results using the image lab software, the expression of the signal-fold degree of each sample was assessed in accordance with the manufacturer's guidelines[25,26].

2.6. Molecular docking investigation

The molecular docking process commenced with a comprehensive examination of five compounds against two specific domains. The analysis focused on two domains in the Caco-2 cell line: the first domain (PDB ID: 7wql), according to Li *et al.*[18], and the second domain (PDB ID: 4bkx), according to Fan *et al.*[20]. The molecular structures of 9-octadecenoic acid, methyl ester (E), hexadecanoic acid, 4H-1-benzopyran-4-one,2-(3,4-dimethoxyphenyl)-3,5-dihydroxy-7-methoxy, oleic acid, and psi,. psi.-carotene, 1,1',2,2'-tetrahydro-1,1'-dimethoxy were processed from the PubChem database (https://pubchem.ncbi.nlm.nih.gov/). An energy minimization study was carried out on each compound using Swiss PDB Viewer software (SPDBV), followed by format conversion from PDB to pdbqt using Open Babel (Version 2.3.1, http://openbabel.org). Subsequent modifications for each enzyme, such as adding hydrogen atoms to the domain and removing water molecules, were performed using Discovery Studio 2019 software[21]. The final step involved preparing the grid box for each domain at 1.00 Å spacing using AutoDock Vina. The grid dimensions were set to 56 Å × 54 Å × 78 Å for the 7wql domain and 70 Å × 72 Å × 60 Å for the 4bkx domain[27].

2.7. Statistical analysis

The acquired data were processed and evaluated using Microsoft Excel. Average inhibitory concentration values and growth curves were analyzed using Origin software. Statistical analysis was performed using one-way ANOVA, followed by Bonferroni *post*

Table 1. Primer sequences.

Gene	Forward sequence	Reverse sequence
Bax	5'-TCAGGATGCGTCCACCAAGAAG-3'	5'- TGTGTCCACGGCGGCAATCATC-3'
TP53	5'-CCTCAGCATCTTATCCGAGTGG-3'	5'-TGGATGGTGGTACAGTCAGAGC-3'
GAPDH	5'-GTCTCCTCTGACTTCAACAGCG-3'	5'- ACCACCCTGTTGCTGTAGCCAA-3'

hoc analysis. A *P* value less than 0.05 was considered statistically significant.

3. Results

3.1. Cytotoxic effect of CCE methanolic extract against HCT116, LoVo, Caco-2, and HT-29 cells

After treatment with different concentrations of the methanolic extract of CCE, we found that the IC_{50} values were (73.065 ± 2.420), (101.159 ± 0.770), (40.370 ± 2.090), and (88.101 ± 3.600) μg/mL, respectively against HCT116, LoVo, Caco-2, and HT-29 cells. Our findings revealed the robust antitumor efficacy of the CCE methanolic extract against these cancer cells, with particularly pronounced activity observed against Caco-2 cells (Figure 1).

3.2. Cytotoxic effect of fractions of CCE methanol extract against Caco-2 cells

The results of this assay revealed that the hexane-dichloromethane mixture (50:50), dichloromethane, dichloromethane-ethyl acetate mixture (50:50), ethyl acetate, ethyl acetate-methanol mixture (50:50), and methanol and acetic acid fractions had variable effects on Caco-2 cell viability, with IC_{50} values of (325.19 ± 34.69), (188.05 ± 14.70), (76.64 ± 0.03), (6.16 ± 0.01), (47.13 ± 1.30), (84.40 ± 6.19), and (218.66 ± 54.30) μg/mL, respectively, while the hexane fraction had no IC_{50} value on Caco-2 cells. Based on the data, the CCE ethyl acetate fraction exhibited the highest efficacy on Caco-2 cell viability and was used for subsequent experiments (Figure 2).

3.3. Identification of the bioactive compounds of CCE by GC-MS analysis

The GC-MS examination of CCE revealed a diverse range of phytocomponents with unique molecular structures and retention times (Supplementary Figure 1). Fifteen components representing 100% of the total fixed oil were identified. Two compounds, 9-octadecenoic acid, methyl ester (E) ($C_{19}H_{36}O_2$) and hexadecanoic acid ($C_{16}H_{32}O_2$), stood out with substantial peak areas of 16.92% and 11.43%, respectively. Betulin ($C_{30}H_{50}O_2$) followed closely at 5.14%. Additionally, lup-20(29)-ene-3,28-diol, (3α) ($C_{30}H_{50}O_2$) constituted 6.49% of the composition.

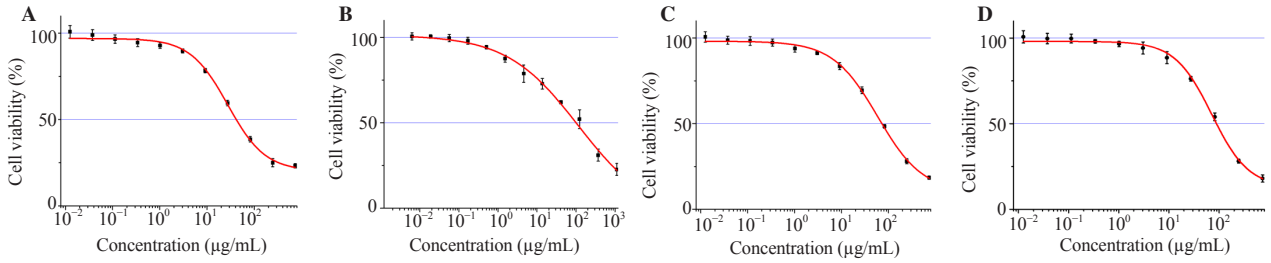


Figure 1. The cytotoxic effect of methanolic extract of *Cymbopogon citratus* on (A) HCT116, (B) LoVo, (C) Caco-2, and (D) HT-29 cell lines using an MTT assay. Data is expressed as mean ± SD (*n*=3).

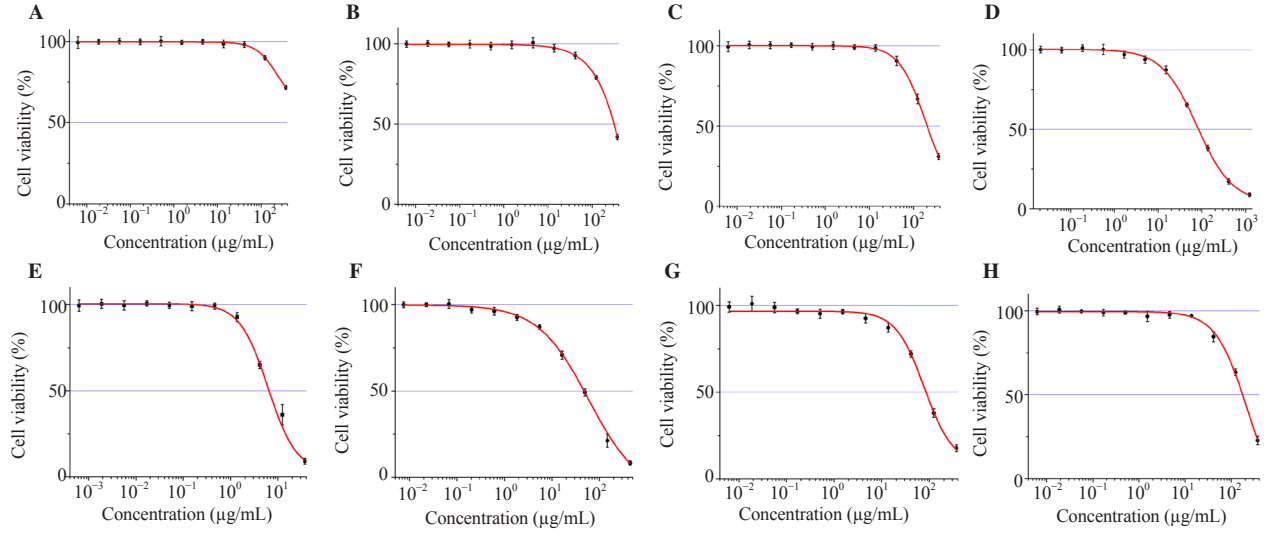


Figure 2. The cytotoxic effect of (A) hexane, (B) hexane + dichloromethane, (C) dichloromethane, (D) dichloromethane + ethyl acetate, (E) ethyl acetate, (F) ethyl acetate + methanol, (G) methanol, and (H) acetic acid fractions of *Cymbopogon citratus* extract on Caco-2 cells using an MTT assay. Data is expressed as mean ± SD (*n*=3).

Various fatty acids and their methyl esters, including oleic acid ($C_{18}H_{34}O_2$), 1,2-benzene dicarboxylic acid ($C_{24}H_{38}O_4$), and stearic acid methyl ester ($C_{19}H_{38}O_2$), were identified, suggesting the presence of lipophilic components contributing to the extract's therapeutic properties. Flavonoids like 4'-OH, 5-OH, 7-*di*-O-glucoside ($C_{27}H_{30}O_{15}$) were detected. Other compounds such as 4H-1-benzopyran-4-one,2-(3,4-dimethoxyphenyl)-3,5-dihydroxy-7-methoxy ($C_{18}H_{16}O_7$) and psi., psi.-carotene, 1,1',2,2'-tetrahydro-1,1'-dimethoxy ($C_{42}H_{64}O_2$) were also found in the extract (Table 2).

3.4. CCE ethyl acetate fraction induces Caco–2 cell apoptosis

The Caco-2 cells in the control group exhibited rounded morphology and green fluorescence, indicating an absence of apoptotic features (Figure 3A). Following 48 hours of treatment with the ethyl acetate fraction of CCE at 1 × IC_{50}, notable nuclear constriction and early apoptotic characteristics became prominent. Moreover, escalating the dosage of the CCE ethyl acetate fraction (2.5 × IC_{50}) resulted in a loss of cell membrane integrity and an augmentation in the number of apoptotic cells. After treatment with

Table 2. Phytocomponents identified in the ethyl acetate fraction of *Cymbopogon citratus* extract by GC-MS analysis.

RT	Compound name	Peak area %	MW (g/mol)	Molecular formula
7.00	Undecane	1.59	156	$C_{11}H_{24}$
25.64	Hexadecanoic acid, methyl ester	4.52	270	$C_{17}H_{34}O_2$
26.44	Hexadecanoic acid	11.43	256	$C_{16}H_{32}O_2$
28.65	9,12-Octadecadienoic acid, methyl ester (E,E)	7.58	294	$C_{19}H_{34}O_2$
28.83	9-Octadecenoic acid, methyl ester (E)	16.92	296	$C_{19}H_{36}O_2$
29.39	Stearic acid methyl ester	3.25	289	$C_{19}H_{38}O_2$
29.63	Oleic acid	8.20	282	$C_{18}H_{34}O_2$
35.82	1,2-Benzenedicarboxylic acid	3.93	390	$C_{24}H_{38}O_4$
40.16	03027205002 flavone,4'-OH,5-OH,7-*di*-*O*-glucoside	2.50	594	$C_{27}H_{30}O_{15}$
41.93	9,12-Octadecadienoic acid(Z,Z)	2.46	489	$C_{27}H_{54}O_4Si_2$
42.19	Betulin	5.14	442	$C_{30}H_{50}O_2$
42.54	Lup-20(29)-ene-3,28-diol, (3α)	6.49	442	$C_{30}H_{50}O_2$
43.08	4H-1-Benzopyran-4-one,2-(3,4-dimethoxyphenyl)-3,5-dihydroxy-7-methoxy	9.30	344	$C_{18}H_{16}O_7$
44.23	4H-1-Benzopyran-4-one, 2-(3,4-dimethoxyphenyl)-3,5	3.70	344	$C_{18}H_{16}O_7$
44.75	psi.,.psi.-Carotene, 1,1',2,2'-tetrahydro-1,1'-dimethoxy	8.26	600	$C_{42}H_{64}O_2$

RT: retention time; MW: molecular weight.

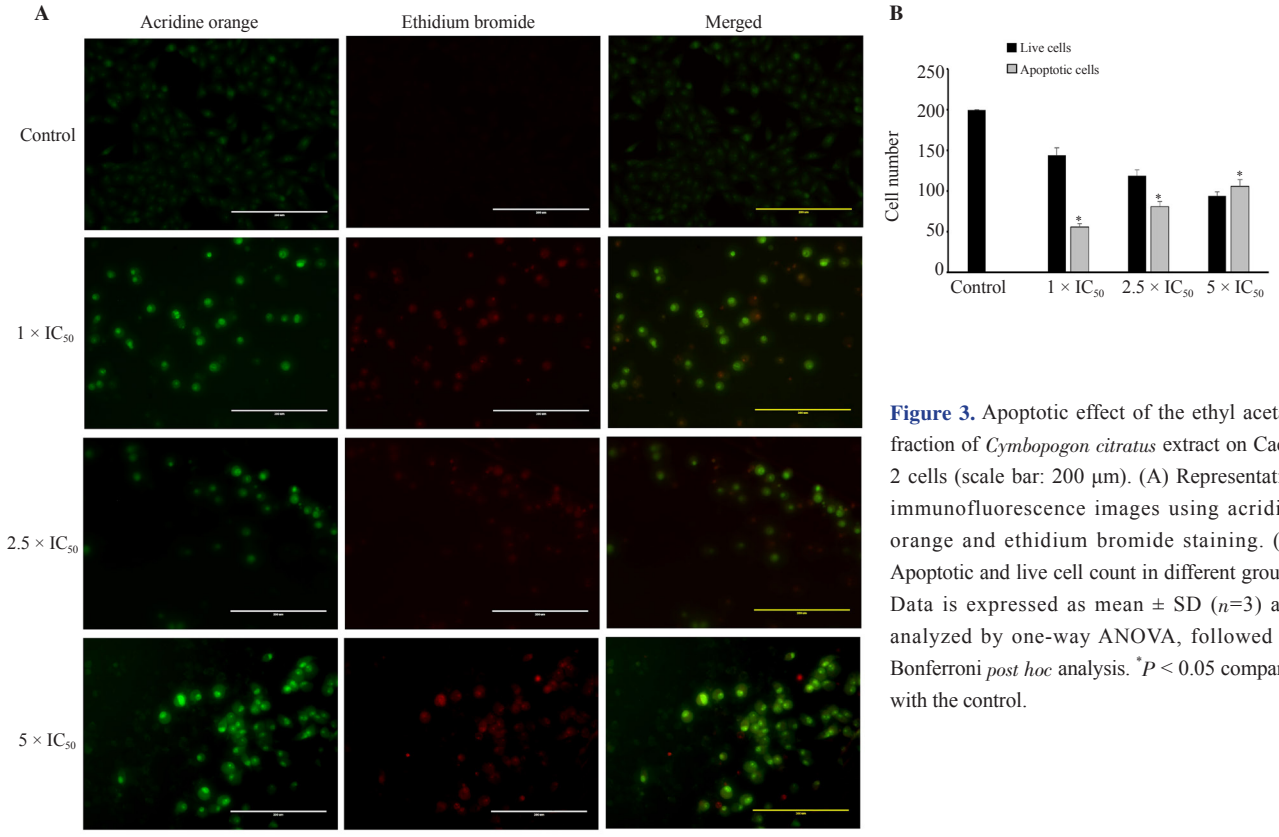


Figure 3. Apoptotic effect of the ethyl acetate fraction of *Cymbopogon citratus* extract on Caco-2 cells (scale bar: 200 μm). (A) Representative immunofluorescence images using acridine orange and ethidium bromide staining. (B) Apoptotic and live cell count in different groups. Data is expressed as mean ± SD (n=3) and analyzed by one-way ANOVA, followed by Bonferroni *post hoc* analysis. $^*P < 0.05$ compared with the control.

an increasing dose of CCE ethyl acetate fraction (5 × IC_{50}), many apoptotic cells appeared compared to the control Caco-2 cells that were not treated with the CCE ethyl acetate fraction. The apoptotic cell percentages of the control group and groups treated with the CCE ethyl acetate fraction at concentrations of 1 × IC_{50}, 2.5 × IC_{50}, and 5 × IC_{50} were (0.17 ± 0.29)%, (29.25 ± 1.77)%, (37.33 ± 3.25)%, and (51.83 ± 5.83)%, respectively (Figure 3B). These data reveal that the CCE ethyl acetate fraction had potent apoptotic effect on Caco-2 cells.

3.5. CCE ethyl acetate fraction upregulates Bax and TP53 expressions in Caco-2 cells

To further evaluate the apoptotic effect of the CCE ethyl acetate fraction, we determined *Bax* and *TP53* gene expression in Caco-2 cells (Figure 4A). Treatment with the CCE ethyl acetate fraction notably upregulated the gene expression of *Bax* in a dose-dependent manner. Moreover, the *TP53* gene expression was significantly increased in cells treated with the CCE ethyl acetate fraction at different concentrations compared to the untreated cells.

3.6. CCE ethyl acetate fraction modulates the expression of apoptosis-related proteins

Figure 4B shows the profile of apoptotic proteins in the Caco-2 cells after exposure to 5 × IC_{50} of CCE ethyl acetate fraction for 24 h. The expressions of Bax, Bid, Bim, Caspase3, Caspase8, DR6, Fas, FasL, p21, p27, and p53 were upregulated in cells treated with the fraction compared to the control (Figure 4B).

3.7. In silico molecular docking results

3.7.1. Binding affinity, hydrophobic residue interactions, and hydrogen bond assessment of docked compounds with the 7wql and 4bkx protein domains

In our extended investigation, we employed molecular docking to

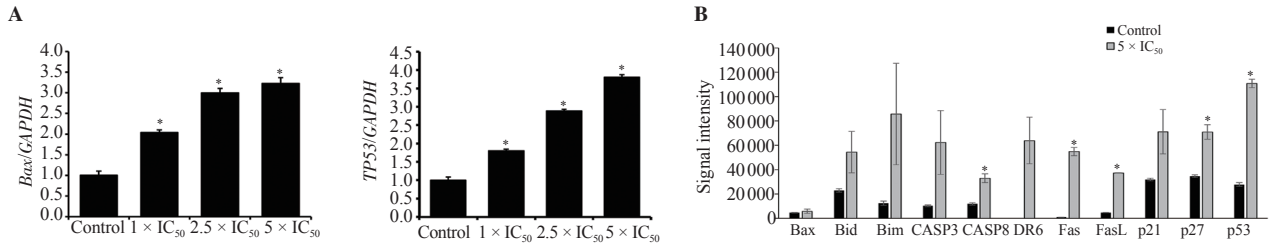


Figure 4. (A) Relative gene expression of *Bax* and *TP53* in Caco-2 cells treated with the ethyl acetate fraction of *Cymbopogon citratus* extract. (B) Apoptotic proteins in Caco-2 cells after treatment with the ethyl acetate fraction of *Cymbopogon citratus* extract [(5 × IC_{50}) μg/mL]. Data is expressed as mean ± SD and analyzed by one-way ANOVA, followed by Bonferroni *post hoc* analysis. $^{*}P < 0.05$ compared with the control.

Table 3. Binding affinity, hydrophobicity, and hydrophilic interactions between docked compounds against the 7wql domain.

Name	Binding affinity (kcal/mol)	Hydrophobic residues	Distance	Hydrophilic interactions	Distance
4H-1-Benzopyran-4-one,2-(3,4-dimethoxyphenyl)-3,5-dihydroxy-7-methoxy	−7.5	LEU133	5.45	ARG148	2.89
		PRO144	5.49	ARG148	2.03
				ARG148	2.51
				GLU134	3.36
psi.,.psi.-Carotene, 1,1',2,2'-tetrahydro-1,1'-dimethoxy	−7.5	ALA23	4.01	ASN152	2.54
		ALA25	4.36	GLU134	3.59
		ARG148	3.55	HIS146	3.70
		LEU140	5.01		
		MET145	4.52		
		ARG148	3.71		
		LYS141	3.80		
		VAL128	5.22		
		VAL128	4.47		
		PRO153	4.37		
		PRO153	5.14		
		PHE136	4.76		
Oleic acid	−5.6	LEU133	5.11	ARG148	2.37
				LEU149	2.83
				LEU149	2.62
9-Octadecenoic acid, methyl ester (E)	−5.4	LYS141	4.44	LEU143:O	3.59
				MET145:O	3.48
Hexadecanoic acid	−5.1	-	-	-	-

validate the activity of five compounds isolated from the CCE ethyl acetate fraction. Specifically, we targeted two domains 7wql and 4bkx of Caco-2 cell line protein. The compounds under investigation include 4H-1-benzopyran-4-one, 2-(3,4-dimethoxyphenyl)-3,5-dihydroxy-7-methoxy; psi.,.psi.carotene,1,1',2,2'-tetrahydro-1,1'-dimethoxy; oleic acid, 9-octadecenoic acid, methyl ester (E); and hexadecanoic acid. Table 3 shows that the binding affinity for ligands ranged from −7.5 kcal/mol [for 4H-1-benzopyran-4-one,2-(3,4-dimethoxyphenyl)-3,5-dihydroxy-7-methoxy and psi.,.psi.-carotene,1,1',2,2'-tetrahydro-1,1'-dimethoxy] to −5.1 kcal/mol (for hexadecanoic acid) against 7wql. In contrast, Table 4 shows that for 4bkx, the binding affinity ranged from −7.1 kcal/mol [for 4H-1-benzopyran-4-one, 2-(3,4-dimethoxyphenyl)-3,5-dihydroxy-7-methoxy] to −6.0 kcal/mol [for 9-octadecenoic acid, methyl ester (E)].

3.7.2. The aromatic interaction and 2D chemical interaction of the docked complexes against the 7wql domain and 4bkx domain of Caco−2 cells

The analysis of aromatic and 2D chemical interactions was conducted on five docked complexes against the 7wql and 4bkx domains sharing the same active site. By delving into the intricacies of aromatic interactions and 2D chemical patterns, the docked complex of 4H-1-benzopyran-4-one, 2-(3,4-dimethoxyphenyl)-3,5-dihydroxy-7-methoxy with 7wql exhibited the most favorable interaction, characterized by the lowest binding energy and the highest number of hydrogen bonds (ARG148, ARG148, ARG148, and GLU134). In contrast, hexadecanoic acid bound to 7wql displayed the weakest chemical interaction. For the 4bkx domain, the docked complex of 4H-1-benzopyran-4-one, 2-(3,4-dimethoxyphenyl)-3,5-dihydroxy-7-methoxy formed the highest number of hydrogen bonds (ARG36, ASP256, ASP332, and TYR15). In contrast, 9-octadecenoic acid, methyl ester (E) exhibited weaker chemical interaction and only one hydrogen bond at HIS253 (Tables 3 and 4).

Next, we elucidated the details of ligand-receptor binding (Supplementary Figure 2), focusing on aspects such as hydrogen bonds (H-bonds), hydrophobic interactions, charges, ionization, and solvent-accessible surface (SAS) interactions, as illustrated in Supplementary Figures 3-5. Supplementary Figure 3J highlights hexadecanoic acid/4bkx, showing the lowest number of hydrogen bonds as donors (pink) and acceptors (green). In contrast, 4H-1-benzopyran-4-one, 2-(3,4-dimethoxyphenyl)-3,5-dihydroxy-7-methoxy/7wql exhibited the highest number of hydrogen bonds as donors and acceptors and featured the most extensive interaction area, predominantly characterized by neutral interactions (Supplementary Figure 3A). Regarding hydrophobicity, the most hydrophilic interaction is illustrated in Supplementary Figure 3M (oleic acid/7wql), whereas the most hydrophobic interaction is shown in Supplementary Figure 3R (oleic acid/4bkx). In terms of charges and ionization, as illustrated in Supplementary Figure 4, the most interactive regions were predominantly negative, as indicated by red color. Specifically, 4H-1-benzopyran-4-one, 2-(3,4-dimethoxyphenyl)-3,5-dihydroxy-7-methoxy/7wql and 4H-1-benzopyran-4-one, 2-(3,4-dimethoxyphenyl)-3,5-dihydroxy-7-methoxy/4bkx exhibited substantial negative charge

Table 4. Binding affinity, hydrophobicity, and hydrophilic interactions between docked compounds against the 4bkx domain.

Name	Binding affinity (kcal/mol)	Hydrophobic residues	Distance	Hydrophilic interactions	Distance
4H-1-Benzopyran-4-one,2-(3,4-dimethoxyphenyl)-3,5-dihydroxy-7-methoxy	−7.1	VAL198	4.94	ARG36	2.09
		ILE249	4.55	ASP256	2.61
				ASP332	3.55
				TYR15	3.28
psi.,.psi.-Carotene, 1,1',2,2'-tetrahydro-1,1'-dimethoxy	−6.9	PRO29	4.13	TYR24	3.46
		LEU271	3.95		
		PRO29	4.57		
		LEU271	5.10		
		PRO29	4.85		
		PRO101	5.10		
		HIS28	4.85		
		HIS141	4.83		
		PHE150	4.41		
		PHE150	5.19		
		HIS178	4.02		
		TYR204	4.92		
		PHE205	4.53		
Hexadecanoic acid	−6.3	VAL198	4.21	ARG36	2.20
		ARG55	4.37		
Oleic acid	−6.1	PHE252	3.74	ARG36	2.44
		TYR15	5.17	ARG36	2.41
				ASN40	2.15
9-Octadecenoic acid, methyl ester (E)	−6.0	VAL198	4.41	HIS253	2.16
		ARG55	4.18		
		HIS253	4.82		

regions (Supplementary Figure 4A and 4F). Conversely, psi,psi-carotene, 1,1',2,2'-tetrahydro-1,1'-dimethoxy/7wql showed a predominance of negative regions in red with minimal positive charge areas depicted in blue (Supplementary Figure 4B). psi,psi-Carotene, 1,1',2,2'-tetrahydro-1,1'-dimethoxy/4bkx primarily demonstrated a neutral charge distribution (Supplementary Figure 4G), while a significant negative charge region was shown in Supplementary Figure 4C. Ionizability is represented in blue, indicating basic complexes and red color denotes acidic complexes. Oleic acid within the 7wql domain showed extensive acidic regions (Supplementary Figure 4M). In contrast, 4H-1-benzopyran-4-one, 2-(3,4-dimethoxyphenyl)-3,5-dihydroxy-7-methoxy and psi,psi-carotene, 1,1',2,2'-tetrahydro-1,1'-dimethoxy within the 4bkx domain exhibited significant expansion of basic regions (Supplementary Figure 4P and 4Q). Additionally, 4H-1-benzopyran-4-one, 2-(3,4-dimethoxyphenyl)-3,5-dihydroxy-7-methoxy demonstrated the majority of the area was acidic (Supplementary Figure 4P). The most substantial SAS interactions in the docked complexes are depicted in blue. Supplementary Figure 5A illustrates this for 4H-1-benzopyran-4-one, 2-(3,4-dimethoxyphenyl)-3,5-dihydroxy-7-methoxy/7wql, while 5J shows the same for hexadecanoic acid/4bkx. Additionally, oleic acid/4bkx and 9-octadecenoic acid, methyl ester (E)/4bkx also display significant SAS interactions (Supplementary Figure 5H and 5I).

4. Discussion

In recent decades, secondary metabolites derived from plant phytochemicals, and their derivatives, have been crucial in combating cancer[10]. In the quest for novel anticancer medications, the National Cancer Institute conducted extensive research on approximately 35 000 plants and 114 000 plant samples from 20 countries[28]. In 2000, researchers observed that 14 of the top 35 cancer-fighting drugs originated from natural sources[11]. The variety of secondary metabolites in plants often results in a broad spectrum of biological activities[29]. *C. citratus* has garnered interest for its diverse phytochemical compounds and therapeutic potential. Its attributes include antioxidant, anticancer, and anti-inflammatory properties, making it a notable natural resource in pharmaceutical research[15]. We evaluated the cytotoxic potential of CCE against cancer cell lines, namely HCT116, LoVo, Caco-2, and HT-29. Notably, the ethyl acetate fraction exhibited a remarkable IC_{50} value of 6.16 μg/mL against Caco-2 cells, establishing it as a particularly promising candidate for further exploration.

Subsequent fractionation of the crude extract yielded eight fractions, each of which demonstrated varying degrees of cytotoxicity against Caco-2 cells. Among these fractions, the ethyl acetate fraction stood out, with a notably potent IC_{50} value of 6.16 μg/mL, underscoring its pronounced efficacy in inhibiting cancer cell growth. Based on this exceptional result, we delve deeper into the composition of this fraction. To unravel the intricate components responsible for its anticancer activity, GC-MS analysis has been employed to identify individual compounds within the ethyl acetate fraction. The analysis of the ethyl acetate fraction using GC-MS has generated a comprehensive profile of bioactive constituents, aiding in the recognition of potential lead compounds with significant anticancer properties.

The diverse components identified, such as essential oils, fatty acids, alcohols, triterpenoids, and flavonoid glycosides, may collectively contribute to the observed cytotoxic activity against Caco-2 cells. Notably, the presence of 9-octadecenoic acid, methyl ester (E), at a concentration of 16.92%, plays a pivotal role as a major constituent in the ethyl acetate fraction. This specific fatty acid derivative significantly enhances the chemical diversity of the fraction, which may potentially exert an impact on the observed anticancer properties. Consistent with our findings, a prior study proposed that targeting fatty acid oxidation in cancer cells could serve as a potential avenue for anticancer treatment. This entails using pharmacological methods to impede cell proliferation, growth, and transformation[30]. Similarly, 9,12-octadecadienoic acid, methyl ester (E,E), with a concentration of 7.58%, has been reported for its notable anticancer activity against a prostate cancer cell line[31].

Lup-20(29)-ene-3,28-diol (3α form) plays a notable role at a concentration of 6.49% in enhancing the bioactive constituents within the ethyl acetate fraction. Previous studies showed that lup-20(29)-ene-3,28-diol reduced nitric oxide production and inhibited TNF-α and IL-1β expression in lipopolysaccharide-stimulated RAW264.7 cells[32]. Further analysis indicated that lup-20(29)-ene-3,28-diol, (3α) could diminish the secretion of high mobility group box 1 (HMGB1), a protein known for its role in inflammation, immune response, and cell signaling. Moreover, the results revealed its efficiency in decreasing NF-κB activation by inhibiting the degradation and phosphorylation of IκBα. NF-κB is a crucial transcription factor involved in regulating immune responses, inflammation, cell proliferation, and survival[32]. Additionally, betulin at a concentration of 5.14% is an abundant triterpene with excellent potential in antioxidant, anti-inflammatory, and anticancer assays[33].

Hexadecanoic acid, a significant compound in the ethyl acetate fraction of CCE, was found in a high concentration of 11.43%. Hexadecanoic acid from *Turbinaria ornata* exhibited a significant 77.83% increase in apoptosis of HT-29 colon cancer, accompanied by a concentration-dependent rise in fluorescence intensity, indicating the formation of reactive oxygen species[34]. Additionally, it impeded the progression of the cell cycle, particularly in the G_0/G_1 phase, where cells typically prepare for DNA replication and division. These findings suggest the potential of hexadecanoic acid as a promising candidate for anticancer therapy[34,35]. Moreover, hexadecanoic acid isolated from red seaweed *Amphiroa zonata*

was investigated for its cytotoxicity against human leukemic cells while sparing normal human dermal fibroblasts[36]. Notably, hexadecanoic acid selectively inhibited DNA topoisomerase Ⅰ activity without impacting DNA topoisomerase Ⅱ function. DNA topoisomerases are crucial enzymes for regulating DNA topology during essential cellular processes, such as replication, transcription, and recombination. DNA topoisomerase Ⅰ relieve torsional stress in DNA strands by inducing single-strand breaks, while DNA topoisomerase Ⅱ can induce double-strand breaks in DNA during replication and transcription. This selective inhibition of DNA topoisomerase Ⅰ by hexadecanoic acid effectively regulates the proliferation of human dermal fibroblasts without harming normal cell viability[37]. In summary, the ethyl acetate fraction is rich in diverse bioactive constituents, particularly concentrated compounds, such as various fatty acids and derivatives. Investigating the complex mechanisms behind the observed cytotoxic effects requires detailed exploration. These compounds not only add complexity to the ethyl acetate fraction's chemical profile, but also significantly contribute to its overall composition, potentially playing crucial roles in the demonstrated cytotoxicity against Caco-2 cells.

Hence, our ongoing research entails comparing the activities of these bioactive compounds with those sourced from the ethyl acetate fractions of CCE. Immunofluorescence staining of cellular organelles has also corroborated cytotoxic effects unveiling apoptotic features in treated cells[38]. EB staining results in dead cells showing red fluorescence, while AO staining results in the DNA/RNA of the cells showing green fluorescence[39]. These dyes are employed in AO/EB staining of Caco-2 cell lines to determine approximate cell viability. Fluorescence microscopy was usually used to observe the treated cells after they were labeled with fluorescent nucleic acid intercalating dyes (AO/EB) in order to identify the nuclear morphological changes and the mechanisms of cell death in Caco-2 cells. When double-stranded DNA is intercalated into the intact membranes of normal cells, the AO dye can pass through and produce green fluorescence. On the other hand, apoptotic cells may have membrane cracks in their nuclei that allow the EB stain to penetrate, producing orange-red fluorescence. Consequently, the AO/EB staining results indicated that CCE could induce apoptosis of Caco-2 cells.

An in-depth exploration of the cellular pathways influenced by the properties of the CCE ethyl acetate fraction included a comprehensive analysis of the transcriptional expression of two essential apoptotic genes, *Bax* and *TP53*, in Caco-2 cells. Bax acknowledged as a pro-apoptotic protein, plays a pivotal role in mitochondrial-mediated apoptosis. Conversely, p53, characterized as a tumor suppressor protein, is well known for its role in regulating cell cycle progression and triggering apoptosis in cells that have suffered damage[40]. The disruption of apoptosis regulation is a distinctive feature of cancer, allowing cells to resist death signals and promote uncontrolled proliferation[41]. Upregulation of proteins involved in the apoptosis pathway, including Bax, Bid, Bim, Caspase3, Caspase8, DR6, Fas, FasL, p21, p27, and p53, was also observed. Triggering apoptosis in cancer cells stands as a pivotal strategy in cancer therapy, and natural products, particularly those sourced from plants, have exhibited the capacity to modulate apoptotic pathways. These findings suggest that compounds derived from plants can influence critical regulators of apoptosis, positioning them as promising compounds for the development of innovative anticancer agents.

A thorough *in silico* molecular docking analysis was carried out using Discovery Studio 2019 software. This computational approach allows the evaluation of binding affinity between small molecules and the targeted protein's binding site, offering valuable insights into the mode of action of pharmacological compounds. The assessment of molecular docking and virtual screening for each domain uncovered the predicted ligand-domain associations, accompanied by their corresponding binding affinity scores and rankings. The first domain, 7wql, exhibited binding affinities ranging from −7.5 kcal/mol to −5.1 kcal/mol for the five compounds. Notably, 4H-1-benzopyran-4-one,2-(3,4-dimethoxyphenyl)-3,5-dihydroxy-7-methoxy displayed the highest binding affinity. Hydrophobic residue interactions were pronounced, especially with psi.,.psi.-carotene,1,1',2,2'-tetrahydro-1,1'-dimethoxy. The strongest hydrogen bond formation occurred with 4H-1-benzopyran-4-one,2-(3,4-dimethoxyphenyl)-3,5-dihydroxy-7-methoxy, indicating robust interaction, while the lowest binding affinity was observed for hexadecanoic acid (−5.1 kcal/mol). The binding affinities of the docked structures showed that each domain formed more stable complexes with the targeted receptors. Analyzing the 2D interactions, all five docked ligands showed interactions at the same active site. However, conventional hydrogen bond and carbon-hydrogen bond analyses highlighted that 4H-1-benzopyran-4-one,2-(3,4-dimethoxyphenyl)-3,5-dihydroxy-7-methoxy formed two conventional hydrogen bonds with the 7wql domain in amino acid residue ARG B:148 and one carbon-hydrogen bond in amino acid residue GLU A:134. Oleic acid displayed robust interactions, establishing three hydrogen bonds (two with LEU B:149 and one with ARG B:149). These compounds demonstrated superior chemical interactions with residues constituting the major binding site, ensuring highly stable complexes. In the 4bkx domain, oleic acid displayed the best chemical interaction with two conventional hydrogen bonds, ASN B:40 and ARG B:30, and 4H-1-benzopyran-4-one,2-(3,4-dimethoxyphenyl)-3,5-dihydroxy-7-methoxy showed strong interaction with two conventional hydrogen bonds, ASP A:256 and ARG B:36, and one carbon-hydrogen bond (TYR B:15). In addition, there were interactions with van der Waals in all the docked complex interactions. These findings underscored the robust chemical interactions of these compounds within the 4bkx domain, indicating stable complex formations.

Hydrogen bonding patterns, illustrated with green representing

acceptors and pink denoting donors, were discernible in the interactions of each compound within the 7wql and 4bkx domains. In the 7wql domain, psi.,.psi.-carotene,1,1',2,2'-tetrahydro-1,1'-dimethoxy showcased a considerable area of acceptor hydrogen bond interactions, surpassing donor interactions. Conversely, 4H-1-benzopyran-4-one,2-(3,4-dimethoxyphenyl)-3,5-dihydroxy-7-methoxy displayed an extensive region of donor hydrogen bond interactions compared to acceptor interactions. Notably, 9-octadecenoic acid, methyl ester (E), being neutral, exhibited limited hydrogen bonding in this domain. Transitioning to the 4bkx domain, the psi.,.psi.-carotene,1,1',2,2'-tetrahydro-1,1'-dimethoxy and hexadecanoic acid complexes demonstrated significant areas of acceptor hydrogen bond interactions, outweighing donor interactions. Conversely, 9-octadecenoic acid, methyl ester (E), displayed a substantial region of donor hydrogen bond interactions compared to acceptor interactions. These findings elucidate distinct hydrogen bonding profiles, suggesting potential implications for the compounds' binding affinities and pharmacological activities. Significantly, these compounds, sourced from CCE, underwent rigorous testing against two specific domains within Caco-2 cells[20]. This rigorous evaluation underscores the compounds' potential relevance and significance in the context of therapeutic investigations.

Charges of docked compounds were color-coded, with negative charges represented in red and positive charges in blue. For the 7wql domain, 4H-1-benzopyran-4-one,2-(3,4-dimethoxyphenyl)-3,5-dihydroxy-7-methoxy and psi., psi.carotene, 1,1',2,2'-tetrahydro-1,1'-dimethoxy displayed a negative charge, suggesting a potential binding affinity with the 7wql domain. Conversely, 9-octadecenoic acid, methyl ester (E), and hexadecanoic acid exhibited neutrality. On the other hand, concerning the 4bkx domain, the docked compounds psi.,.psi.-carotene,1,1',2,2'-tetrahydro-1,1'-dimethoxy, hexadecanoic acid, and oleic acid appeared neutral, while 4H-1-benzopyran-4-one,2-(3,4-dimethoxyphenyl)-3,5-dihydroxy-7-methoxy displayed a negative charge. Similarly, the ionizability was shown in blue for the basic complex and red for the acidic complex. The hydrophobic area, shown in brown, increased with oleic acid in the 7wql domain. Concurrently, an enlargement of the hydrophobic region was noted for 4H-1-benzopyran-4-one,2-(3,4-dimethoxyphenyl)-3,5-dihydroxy-7-methoxy and psi.,.psi.-carotene,1,1',2,2'-tetrahydro-1,1'-dimethoxy within the 4bkx domain. These alterations signify a robust intensification of hydrophobic interactions, indicating a potent inhibitory effect and substantial binding strength. The SAS was depicted in blue for each interaction of the docked complexes, a color that was consistently heightened across all docked complexes[42]. While our study presents significant findings, several limitations should be acknowledged. First, our evaluation was based on a limited selection of cell lines, which may not fully represent the diversity of cancer types and responses. Additionally, our investigation was confined to *in vitro* assays, leaving the *in vivo* efficacy and safety of the ethyl acetate fraction unexplored. We focused specifically on the ethyl acetate fraction, potentially missing contributions from other components within the crude extract. While our molecular docking studies provide promising insights into binding affinities, these predictions require experimental validation for confirmation. Despite these limitations, the study's findings are a valuable step forward, highlighting the potential of the ethyl acetate fraction for further investigation and development as an anticancer agent. Future research should address these gaps to fully understand and validate the therapeutic potential of CCE.

In conclusion, this study demonstrates the anticancer potential of CCE, particularly its ethyl acetate fraction, through a series of detailed evaluations. The methanolic extract exhibited significant cytotoxicity across various colorectal cancer cell lines, with the Caco-2 cell line showing the highest sensitivity. Among the fractions tested, the ethyl acetate fraction was the most effective, exhibiting a notably low IC_{50} value against Caco-2 cells. GC-MS analysis identified key bioactive compounds, including 9-octadecenoic acid and hexadecanoic acid, which may contribute to the observed cytotoxic effects. The ethyl acetate fraction also induced apoptosis in Caco-2 cells, as evidenced by immunofluorescence staining and gene expression analysis, which showed increased levels of *Bax* and *TP53*. Additionally, the protein array results confirmed the upregulation of several apoptosis-related proteins in treated cells. Molecular docking studies further revealed that the compounds from CCE interact effectively with key protein domains, supporting their potential therapeutic mechanisms. Overall, these findings underscore the significant anticancer activity of CCE and its potential for further development as a natural cancer treatment. This study provides the groundwork for future investigations and advancements in plant-derived treatments for colorectal cancer.

Conflict of interest statement

The authors declare no conflict of interest.

Acknowledgments

The authors extend their appreciation to Researchers Supporting Project number (RSP2025R414) King Saud University, Riyadh, Saudi Arabia.

Funding

This work was supported by Researchers Supporting Project number (RSP2025R414) King Saud University, Riyadh, Saudi Arabia.

Data availability statement

The data supporting the findings of this study are available from the corresponding authors upon request.

Authors' contributions

All authors contributed to the study's conception and design. Material preparation, data collection, and analysis were performed by BA, MA, BAD, and AR. The first draft of the manuscript was written by BA and all authors commented on previous versions of the manuscript. All authors read and approved the final manuscript.

References

[1] Soerjomataram I, Bray F. Planning for tomorrow: Global cancer incidence and the role of prevention 2020-2070. *Nat Rev Clin Oncol* 2021; **18**(10): 663-672.

[2] World Health Organization. World Health Statistics 2016: Monitoring health for the sustainable development goals (SDGs). [Online] Available from: https://www.who.int/publications/i/item/9789241565264 [Accessed on December 12, 2023].

[3] Wong MC, Huang J, Lok V, Wang J, Fung F, Ding H, et al. Differences in incidence and mortality trends of colorectal cancer worldwide based on sex, age, and anatomic location. *Clin Gastroenterol Hepatol* 2021; **19**(5): 955-966.

[4] Sawicki T, Ruszkowska M, Danielewicz A, Niedźwiedzka E, Arłukowicz T, Przybyłowicz KE. A review of colorectal cancer in terms of epidemiology, risk factors, development, symptoms and diagnosis. *Cancers (Basel)* 2021; **13**(9). doi: 10.3390/cancers13092025.

[5] Greenwell M, Rahman P. Medicinal plants: Their use in anticancer treatment. *Int J Pharm Sci Res* 2015; **6**(10). doi: 10.13040%2FIJPSR.0975-8232.6(10).4103-12.

[6] Khan T, Ali M, Khan A, Nisar P, Jan SA, Afridi S, et al. Anticancer plants: A review of the active phytochemicals, applications in animal models, and regulatory aspects. *Biomolecules* 2019; **10**(1). doi: 10.3390/biom10010047.

[7] Cooper GM, Hausman R. *The cell: A molecular approach.* USA: Oxford University Press: Sinauer Associates; 2000, p. 719-728.

[8] Kumar S, Pathania AS, Saxena A, Vishwakarma R, Ali A, Bhushan S. The anticancer potential of flavonoids isolated from the stem bark of *Erythrina suberosa* through induction of apoptosis and inhibition of STAT signaling pathway in human leukemia HL-60 cells. *Chem Biol Interact* 2013; **205**(2): 128-137.

[9] Mosmann T. Rapid colorimetric assay for cellular growth and survival: Application to proliferation and cytotoxicity assays. *J Immunol Methods* 1983; **65**(1-2): 55-63.

[10]Atanasov AG, Zotchev SB, Dirsch VM, Supuran CT. Natural products in drug discovery: Advances and opportunities. *Nat Rev Drug Discov* 2021; **20**(3): 200-216.

[11]Talib WH, Alsalahat I, Daoud S, Abutayeh RF, Mahmod AI. Plant-derived natural products in cancer research: Extraction, mechanism of action, and drug formulation. *Molecules* 2020; **25**(22). doi: 10.3390/molecules25225319.

[12]Aftab K, Ali M, Aijaz P, Beena N, Gulzar H, Sheikh K, et al. Determination of different trace and essential element in lemon grass samples by X-ray fluorescence spectroscopy technique. *Int Food Res J* 2011; **18**(1): 265-270.

[13]Ajayi E, Sadimenko A, Afolayan A. GC-MS evaluation of *Cymbopogon citratus* (DC) Stapf oil obtained using modified hydrodistillation and microwave extraction methods. *Food Chem* 2016; **209**: 262-266.

[14]Chen H, Zhu B, Zhao L, Liu Y, Zhao F, Feng J, et al. Allicin inhibits proliferation and invasion *in vitro* and *in vivo via* SHP-1-mediated STAT3 signaling in cholangiocarcinoma. *Cell Physiol Biochem* 2018; **47**(2): 641-653.

[15]Oladeji OS, Adelowo FE, Ayodele DT, Odelade KA. Phytochemistry and pharmacological activities of *Cymbopogon citratus*: A review. *Sci Afr* 2019; **6**. doi: 10.1016/j.sciaf.2019.e00137.

[16]Karkala Manvitha KM, Bhushan Bidya BB. Review on pharmacological activity of *Cymbopogon citratus*. *Int J Herb Med* 2014; **1**(6): 5-7.

[17]Toropov O. Electron ionization library component of the NIST/EPA/NIH Mass Spectral Library and NIST GC Retention Index Database. [Online] Available from: https://www.nist.gov/programs-projects/electron-ionization-library-component-nistepanih-mass-spectral-library-and-nist-gc [Accessed on December 18, 2023].

[18]Li T, Jiao R, Ma J, Zang J, Zhao G, Zhang T. Zinc binding strength of proteins dominants zinc uptake in Caco-2 cells. *RSC adv* 2022; **12**(33): 21122-21128.

[19]Liu K, Liu PC, Liu R, Wu X. Dual AO/EB staining to detect apoptosis in osteosarcoma cells compared with flow cytometry. *Med Sci Monit Basic Res* 2015; **21**: 15-20.

[20]Fan X, Guo H, Teng C, Zhang B, Blecker C, Ren G. Anti-colon cancer activity of novel peptides isolated from *in vitro* digestion of quinoa protein in Caco-2 cells. *Foods* 2022; **11**(2). doi: 10.3390/foods11020194.

[21]Umar HI, Saliu TP, Josiah SS, Ajayi A, Danjuma JB. *In silico* studies of bioactive compounds from selected African plants with inhibitory activity against nitric oxide synthase and arginase implicated in asthma. *Egypt J Med Hum Genet* 2021; **22**: 1-16.

[22]Avoseh O, Oyedeji O, Rungqu P, Nkeh-Chungag B, Oyedeji A. *Cymbopogon* species; ethnopharmacology, phytochemistry and the pharmacological importance. *Molecules* 2015; **20**(5): 7438-7453.

[23]Almutairi BO, Almutairi MH, Alrefaei AF, Alkahtani S, Alarifi S. HSPB6 is depleted in colon cancer patients and its expression is induced by 5-aza-2′-deoxycytidine *in vitro*. *Medicina* 2023; **59**(5). doi: 10.3390/medicina59050996.

[24]Bradford MM. A rapid and sensitive method for the quantitation of microgram quantities of protein utilizing the principle of protein-dye binding. *Anal Biochem* 1976; **72**(1-2): 248-254.

[25]Almutairi BO, Almutairi SM, Alarifi S. Synthesis of 1-(4-chlorobenzoyl)-

4-(dimethylamino) pyridin-1-ium chloride and determination of cytotoxicity and apoptosis in human colon cancer cells. *J King Saud Univ Sci* 2024; **36**(3). doi: 10.1016/j.jksus.2024.103101.

[26]Ferrer RJ, Ong MJ, Jacinto SD. Extract of *Codiaeum luzonicum* Merr. overcomes multidrug resistance in human colon cancer cells by modulating *P*-glycoprotein. *Asian Pac J Trop Biomed* 2022; **12**(9): 400-410.

[27]Labib MM, Amin M, Alzohairy A, Elashtokhy M, Samir O, Hassanein S. Inhibition analysis of aflatoxin by *in silico* targeting the thioesterase domain of polyketide synthase enzyme in *Aspergillus* ssp. *J Biomol Struct Dyn* 2022; **40**(10): 4328-4340.

[28]Shoeb M. Anti-cancer agents from medicinal plants. *Bangladesh J Pharmacol* 2006; **1**(2): 35-41.

[29]Kumar S, Korra T, Thakur R, Arutselvan R, Kashyap AS, Nehela Y, et al. Role of plant secondary metabolites in defence and transcriptional regulation in response to biotic stress. *Plant Stress* 2023; **8**. doi: 10.1016/j.stress.2023.100154.

[30]Jin Z, Chai YD, Hu S. Fatty acid metabolism and cancer. *Adv Exp Med Biol* 2021; **1280**: 231-241.

[31]Ukwubile C, Ahmed A, Katsayal U, Ya'u J, Mejida S. GC-MS analysis of bioactive compounds from *Melastomastrum capitatum* (Vahl) Fern. leaf methanol extract: An anticancer plant. *Sci Afr* 2019; **3**. doi: 10.1016/j.sciaf.2019.e00059.

[32]Liu XQ, Zou QP, Huang JJ, Yook CS, Whang WK, Lee HK, et al. Inhibitory effects of 3α-hydroxy-lup-20 (29)-en-23, 28-dioic acid on lipopolysaccharide-induced TNF-α, IL-1β, and the high mobility group box 1 release in macrophages. *Biosci Biotechnol Biochem* 2017; **81**(7): 1305-1313.

[33]Kaur P, Arora S, Singh R. Isolation, characterization and biological activities of betulin from *Acacia nilotica* bark. *Sci Rep* 2022; **12**(1). doi: 10.1038/s41598-022-13338-3.

[34]Bharath B, Perinbam K, Devanesan S, AlSalhi MS, Saravanan M. Evaluation of the anticancer potential of hexadecanoic acid from brown algae *Turbinaria ornata* on HT-29 colon cancer cells. *J Mol Struct* 2021; **1235**. doi: 10.1016/j.molstruc.2021.130229.

[35]Kumari R, Sharma N, Karwasra R, Khanna K. Colon cancer and their targeting approaches through nanocarriers: A review. *Asian Pac J Trop Biomed* 2023; **13**(3): 104-111.

[36]Harada H, Yamashita U, Kurihara H, Fukushi E, Kawabata J, Kamei Y. Antitumor activity of palmitic acid found as a selective cytotoxic substance in a marine red alga. *Anticancer Res* 2002; **22**(5): 2587-2590.

[37]Kasibhatla S, Amarante-Mendes GP, Finucane D, Brunner T, Bossy-Wetzel E, Green DR. Acridine orange/ethidium bromide (AO/EB) staining to detect apoptosis. *Cold Spring Harbor Protocols* 2006; **2006**(3). doi: 10.1101/pdb.prot4493.

[38]Im K, Mareninov S, Diaz MFP, Yong WH. An introduction to performing immunofluorescence staining. *Methods Mol Biol* 2019; **1897**: 299-311.

[39]Shinde V, Desai K. *In vitro* cytotoxicity, macromolecular interaction and antioxidant potential of dual coated selenium nanoparticles. *J Biomed Mater Res B* 2022; **110**(6): 1400-1411.

[40]Peña-Blanco A, García-Sáez AJ. Bax, Bak and beyond—mitochondrial performance in apoptosis. *FEBS J* 2018; **285**(3): 416-431.

[41]Carneiro BA, El-Deiry WS. Targeting apoptosis in cancer therapy. *Nat Rev Clin Oncol* 2020; **17**(7): 395-417.

[42]Imbabi TA, Habashy WS, Abol-Fetouh GM, Labib MM, Osman A, Elkelish A, et al. Enhancing semen quality, brain neurotransmitters, and antioxidant status of rabbits under heat stress by acacia gum, vitamin C, and lycopene as dietary supplements: An *in vitro* and *in silico* study. *Ital J Anim Sci* 2023; **22**(1): 321-336.

Publisher's note

The Publisher of the *Journal* remains neutral with regard to jurisdictional claims in published maps and institutional affiliations.

Edited by Liang Q, Tan BJ

Phytochemical profiling and anticancer potential of *Cymbopogon citratus* extract

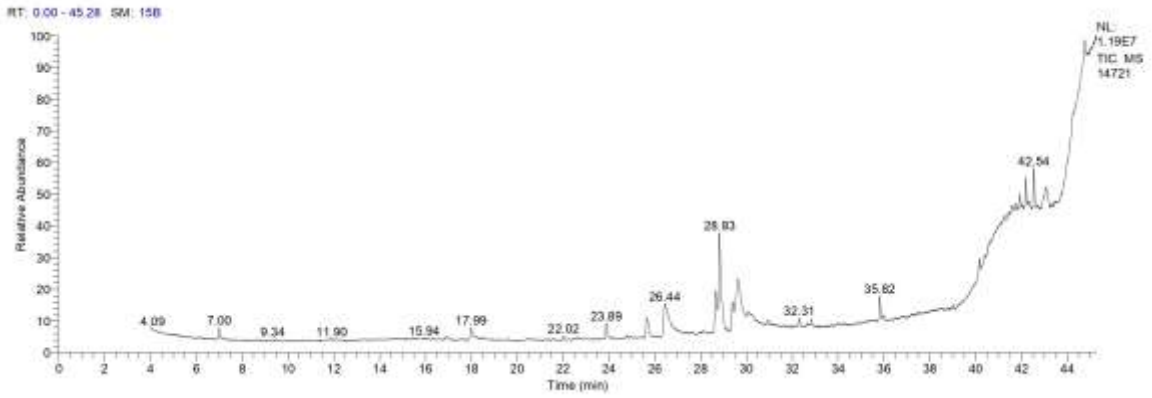
Running title: Anticancer properties of Cymbopogon citratus extract

Bader O. Almutairi*, Mikhlid H. Almutairi, Badr A. Al-Dahmash, Saad Alkahtani, Saud Alarifi, Ahmed Rady*

Department of Zoology, College of Science, King Saud University, P.O. Box 2455, Riyadh 11451, Saudi Arabia

* Corresponding Authors:

E-mail addresses: bomotairi@ksu.edu.sa (B.O. Almutairi) +966 55 266 8778, ahabdo@ksu.edu.sa (Ahmed Rady) +966 54 642 9800.



Supplementary Figure 1. Chromatographic elution profile for GC-MS analysis of Cymbopogon citratus extract.

Phytochemical profiling and anticancer potential of *Cymbopogon citratus* extract

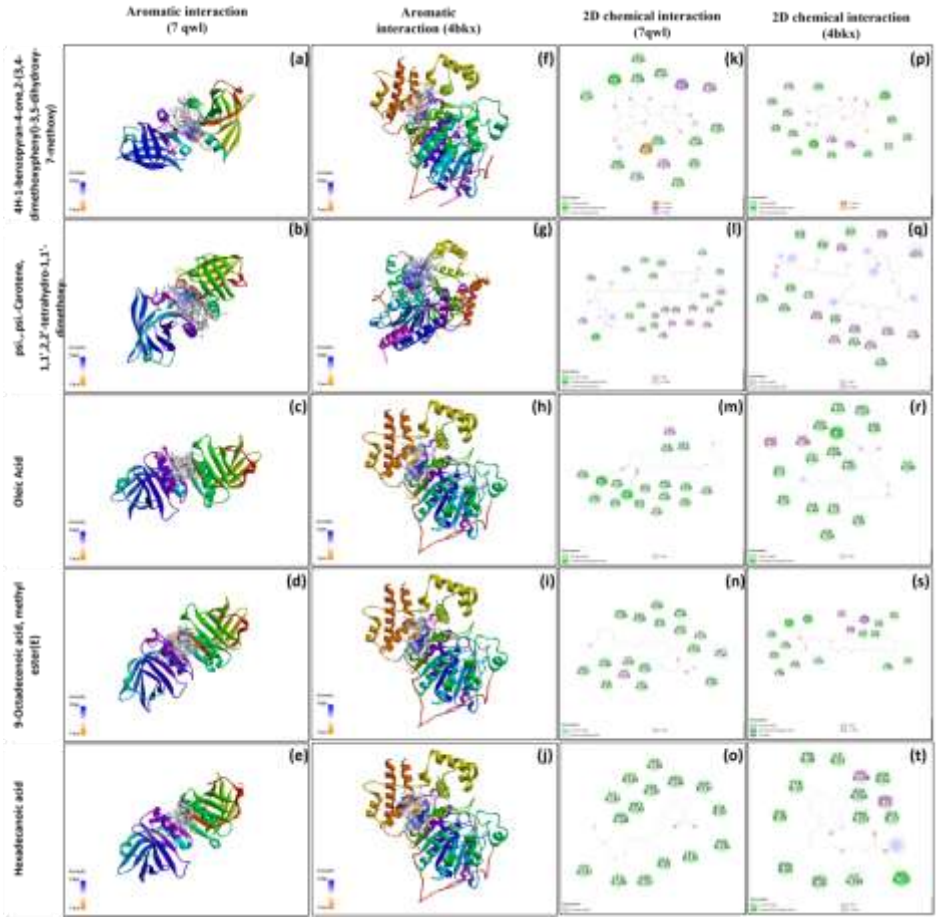
Running title: Anticancer properties of Cymbopogon citratus extract

Bader O. Almutairi*, Mikhlid H. Almutairi, Badr A. Al-Dahmash, Saad Alkahtani, Saud Alarifi, Ahmed Rady*

Department of Zoology, College of Science, King Saud University, P.O. Box 2455, Riyadh 11451, Saudi Arabia

* Corresponding Authors:

E-mail addresses: bomotairi@ksu.edu.sa (B.O. Almutairi) +966 55 266 8778, ahabdo@ksu.edu.sa (Ahmed Rady) +966 54 642 9800.



Supplementary Figure **2.** Aromatic interaction and 2D chemical interaction of docked compounds with 7wql: **(A)** 4H-1-benzopyran-4-one,2-(3,4-dimethoxyphenyl)-3,5-dihydroxy-7-methoxy**, (B)** psi.,.psi.-carotene,1,1',2,2'-tetrahydro-1,1'-dimethoxy, **(C)** oleic acid, **(D)** 9-octadecenoic acid, methyl ester (E), and **(E)** hexadecanoic acid. Aromatic interaction of docked compound with 4bkx: **(F)** 4H-1-benzopyran-4-one,2-(3,4-dimethoxyphenyl)-3,5-dihydroxy-7-methoxy, **(G)** psi.,.psi.-carotene,1,1',2,2'-tetrahydro-1,1'-dimethoxy, **(H)** oleic acid, **(I)** 9-octadecenoic acid, methyl ester (E), and **(J)** hexadecanoic acid. 2D chemical interaction of docked compound with 7wql: **(K)** 4H-1-benzopyran-4-one,2-(3,4-dimethoxyphenyl)-3,5-dihydroxy-7-methoxy, **(L)** psi.,.psi.-carotene,1,1',2,2'-tetrahydro-1,1'-dimethoxy, **(M)** oleic acid, **(N)** 9-octadecenoic acid, methyl ester (E), and **(O)** hexadecanoic acid. 2D chemical interaction of docked compounds with 4bkx: **(P)** 4H-1-benzopyran-4-one,2-(3,4-dimethoxyphenyl)-3,5-dihydroxy-7-methoxy, **(Q)** psi.,.psi.-carotene,1,1',2,2'-tetrahydro-1,1'-dimethoxy, **(R)** oleic acid, **(S)** 9-octadecenoic acid, methyl ester (E), and **(T)** hexadecanoic acid.

Phytochemical profiling and anticancer potential of *Cymbopogon citratus* extract

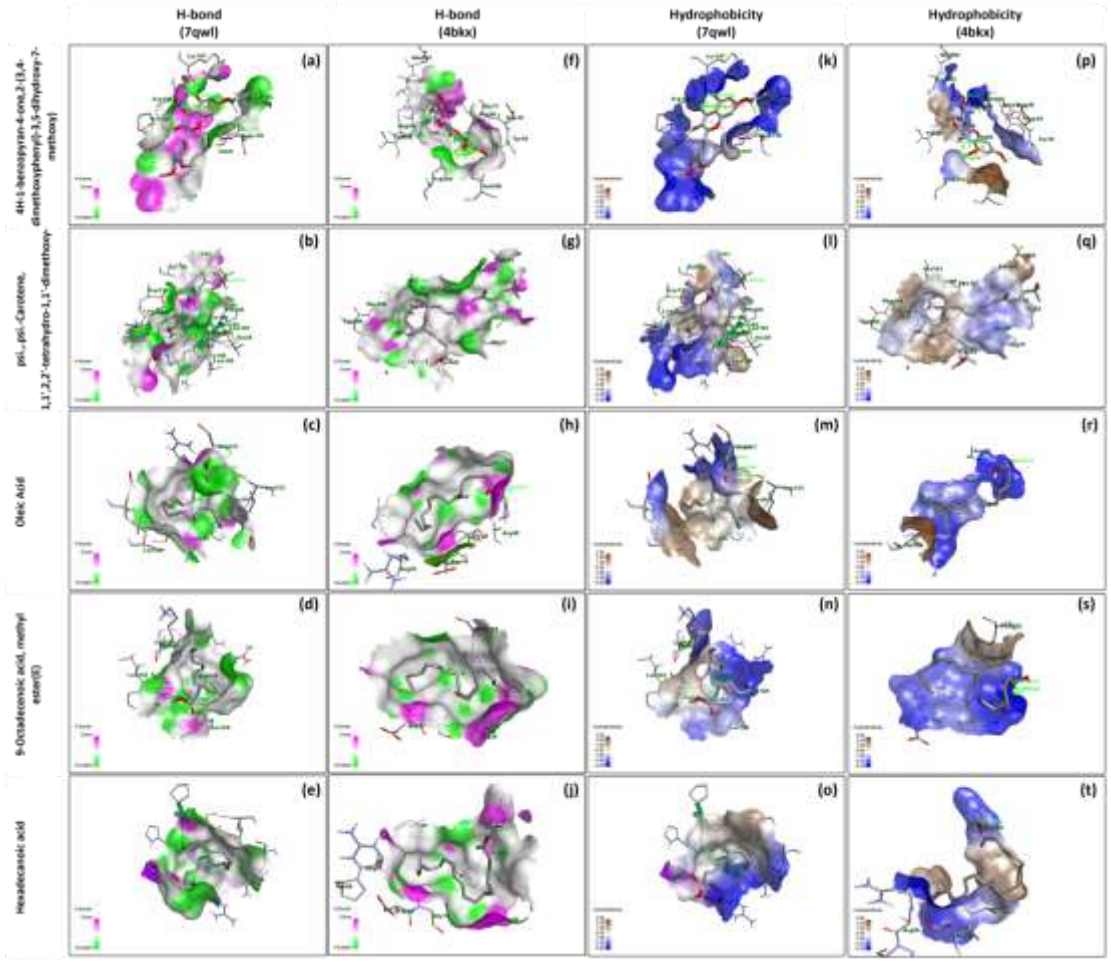
Running title: Anticancer properties of Cymbopogon citratus extract

Bader O. Almutairi*, Mikhlid H. Almutairi, Badr A. Al-Dahmash, Saad Alkahtani, Saud Alarifi, Ahmed Rady*

Department of Zoology, College of Science, King Saud University, P.O. Box 2455, Riyadh 11451, Saudi Arabia

* Corresponding Authors:

E-mail addresses: bomotairi@ksu.edu.sa (B.O. Almutairi) +966 55 266 8778, ahabdo@ksu.edu.sa (Ahmed Rady) +966 54 642 9800.



Supplementary Figure **3.** Representations of the H-bond and hydrophobicity of docked compounds and two domains. H-bond for 7qwl: **(A)** 4H-1-benzopyran-4-one,2-(3,4-dimethoxyphenyl)-3,5-dihydroxy-7-methoxy, **(B)** psi.,.psi.-carotene,1,1',2,2'-tetrahydro-1,1'-dimethoxy, **(C)** oleic acid, **(D)** 9-octadecenoic acid, methyl ester (E), and **(E)** hexadecanoic acid. H-bond for 4bkx: **(F)** 4H-1-benzopyran-4-one,2-(3,4-dimethoxyphenyl)-3,5-dihydroxy-7-methoxy, **(G)** psi.,.psi.-xcarotene,1,1',2,2'-tetrahydro-1,1'-dimethoxy, **(H)** oleic acid, **(I)** 9-octadecenoic acid, methyl ester (E), and **(J)** hexadecanoic acid. Hydrophobicity of 7wql: **(K)** 4H-1-benzopyran-4-one,2-(3,4-dimethoxyphenyl)-3,5-dihydroxy-7-methoxy, **(L)** psi.,.psi.-carotene,1,1',2,2'-tetrahydro-1,1'-dimethoxy, **(M)** oleaic acid, **(N)** 9 -Octadecenoic acid, methyl ester (E)**, (O)** hexadecanoic acid. Hhydrophobicity of 4bkx: **(P)** 4H-1-benzopyran-4-one,2-(3,4-dimethoxyphenyl)-3,5-dihydroxy-7-methoxy, **(Q)** psi.,.psi.-Carotene,1,1',2,2'-tetrahydro-1,1'-dimethoxy, **(R)** oleic acid, **(S)** 9 -octadecenoic acid, and **(T)** hexadecanoic acid.

Phytochemical profiling and anticancer potential of *Cymbopogon citratus* extract

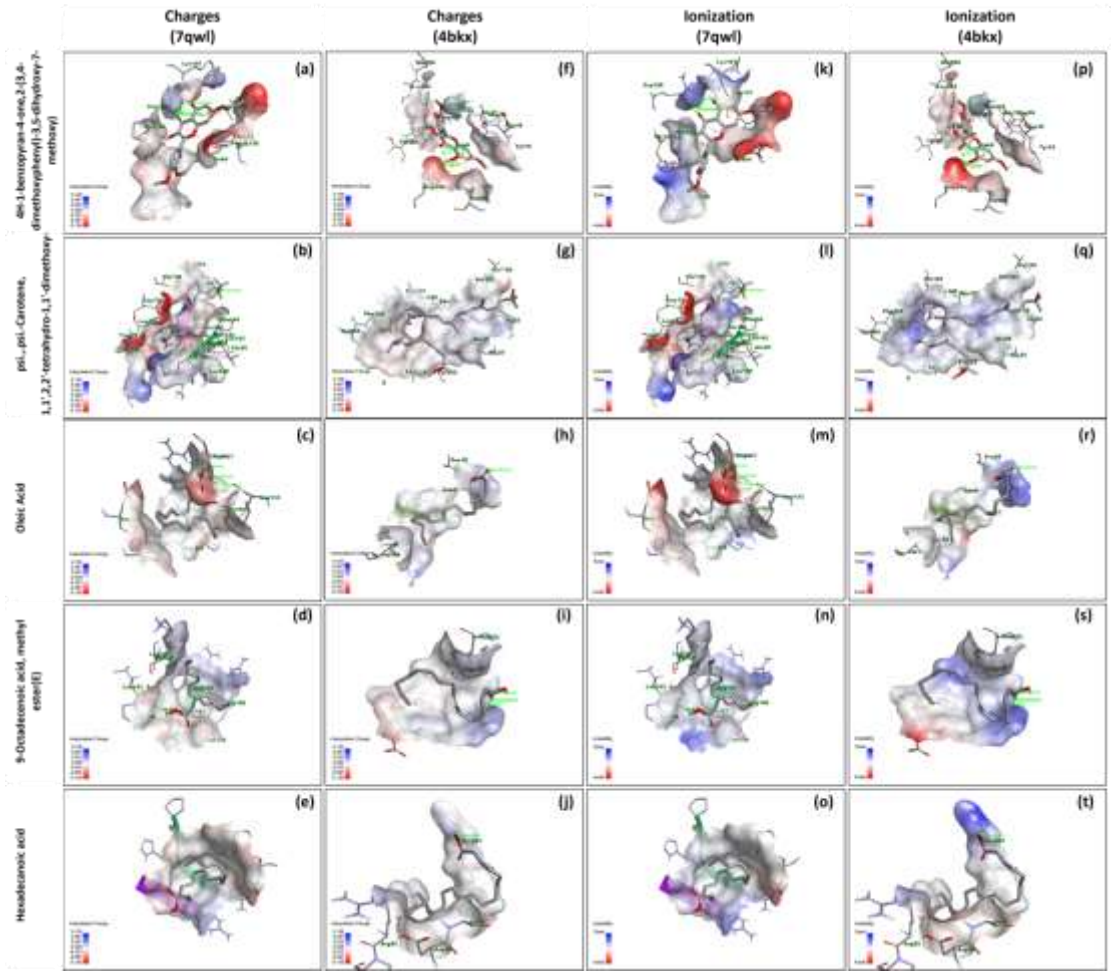
Running title: Anticancer properties of Cymbopogon citratus extract

Bader O. Almutairi*, Mikhlid H. Almutairi, Badr A. Al-Dahmash, Saad Alkahtani, Saud Alarifi, Ahmed Rady*

Department of Zoology, College of Science, King Saud University, P.O. Box 2455, Riyadh 11451, Saudi Arabia

* Corresponding Authors:

E-mail addresses: bomotairi@ksu.edu.sa (B.O. Almutairi) +966 55 266 8778, ahabdo@ksu.edu.sa (Ahmed Rady) +966 54 642 9800.



Supplementary Figure 4. Representations of charges and ionization of docked compounds and two targeted domains for 7wql: **(A)** 4H-1-benzopyran-4-one,2-(3,4-dimethoxyphenyl)-3,5-dihydroxy-7-methoxy, **(B)** psi.,.psi.-carotene,1,1',2,2'-tetrahydro-1,1'-dimethoxy, **(C)** oleic acid, **(D)** 9-octadecenoic acid, methyl ester (E), and **(E)** hexadecanoic acid. For 4bkx: **(F)** 4H-1-benzopyran-4-one,2-(3,4-dimethoxyphenyl)-3,5-dihydroxy-7-methoxy, **(G)** psi.,.psi.-carotene,1,1',2,2'-tetrahydro-1,1'-dimethoxy, **(H)** oleic acid, **(I)** 9-octadecenoic acid, methyl ester (E), and **(J)** hexadecanoic acid. For ionization of 7qwl: **(K)** 4H-1-benzopyran-4-one,2-(3,4-dimethoxyphenyl)-3,5-dihydroxy-7-methoxy, **(L)** psi.,.psi.-carotene,1,1',2,2'-tetrahydro-1,1'-dimethoxy, **(M)** oleic acid, **(N)** 9-octadecenoic acid, methyl ester (E), and **(O)** hexadecanoic acid. For ionization of 4bkx, **(P)** 4H-1-benzopyran-4-one,2-(3,4-dimethoxyphenyl)-3,5-dihydroxy-7-methoxy, **(Q)** psi.,.psi.-carotene,1,1',2,2'-tetrahydro-1,1'-dimethoxy, **(R)** oleic acid, **(S)** 9-octadecenoic acid, methyl ester (E), and **(T)** hexadecanoic acid.

Phytochemical profiling and anticancer potential of *Cymbopogon citratus* extract

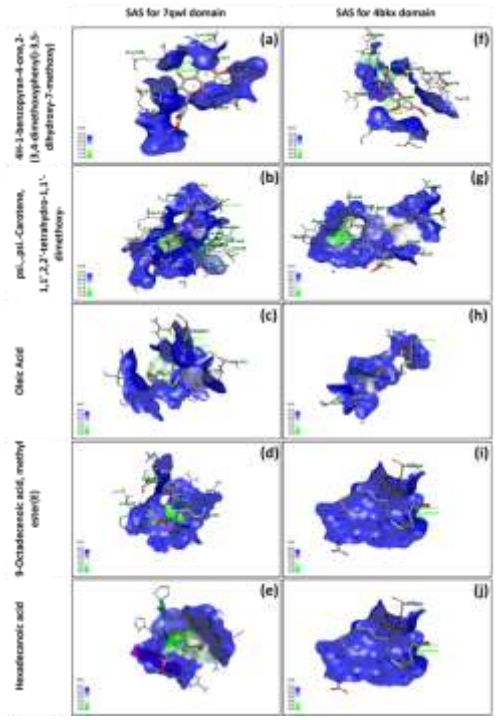
Running title: Anticancer properties of Cymbopogon citratus extract

Bader O. Almutairi*, Mikhlid H. Almutairi, Badr A. Al-Dahmash, Saad Alkahtani, Saud Alarifi, Ahmed Rady*

Department of Zoology, College of Science, King Saud University, P.O. Box 2455, Riyadh 11451, Saudi Arabia

* Corresponding Authors:

E-mail addresses: bomotairi@ksu.edu.sa (B.O. Almutairi) +966 55 266 8778, ahabdo@ksu.edu.sa (Ahmed Rady) +966 54 642 9800.



Supplementary Figure **5**. Representations of solvent accessible surface (SAS) of docked ligand with two targeted domains: For 7qwl: **(A)** 4H-1-benzopyran-4-one,2-(3,4-dimethoxyphenyl)-3,5-dihydroxy-7-methoxy, **(B)** psi.,.psi.-carotene,1,1',2,2'-tetrahydro-1,1'-dimethoxy, **(C)** oleic acid, **(D)** 9-octadecenoic acid, methyl ester (E), and **(E)** hexadecanoic acid; For 4bkx: **(F)** 4H-1-benzopyran-4-one,2-(3,4-dimethoxyphenyl)-3,5-dihydroxy-7-methoxy, **(G)** psi.,.psi.-carotene,1,1',2,2'-tetrahydro-1,1'-dimethoxy, **(H)** oleic acid, **(I)** 9-octadecenoic acid, methyl ester (E), and **(J)** hexadecanoic acid.